Timed mutation and cell-fate mapping reveal reiterated roles of *Tbx1* during embryogenesis, and a crucial function during segmentation of the pharyngeal system via regulation of endoderm expansion

Huansheng Xu[1,2,3], Fabiana Cerrato[3] and Antonio Baldini[1,2,3,4,*]

[1]Program in Cardiovascular Sciences, Baylor College of Medicine, Houston, TX 77030, USA
[2]Center for Cardiovascular Development, Baylor College of Medicine, Houston, TX 77030, USA
[3]Departments of Pediatrics (Cardiology), Baylor College of Medicine, Houston, TX 77030, USA
[4]Molecular and Human Genetics, Baylor College of Medicine, Houston, TX 77030, USA
*Author for correspondence (e-mail: baldini@bcm.tmc.edu)

Accepted 29 July 2005

Development 132, 4387-4395
Published by The Company of Biologists 2005
doi:10.1242/dev.02018

Summary

The definition of time-specific requirements for a developmental gene can pinpoint the processes within which the gene is involved and can reveal potential late functions in structures and organs that fail to develop in germline mutants. Here, we show the first systematic time-course deletion, in parallel with timed cell fate mapping, of a developmentally crucial gene, *Tbx1*, during mouse embryogenesis. *Tbx1* mouse mutants model DiGeorge syndrome, a disorder of pharyngeal and cardiovascular development. Results revealed different time requirements for the development of individual structures, as well as multiple and time-distinct roles during the development of the same organ or system. We also show that *Tbx1* is required throughout pharyngeal segmentation for the regulation of endoderm expansion, thus this is the first gene implicated directly in this process. A genetic-based blueprint of crucial developmental times for organs and systems should be a valuable asset for our understanding of birth defect pathogenesis.

Key words: *Tbx1*, Timed mutation, DiGeorge syndrome

Introduction

Tbx1 encodes a transcription factor belonging to the T-box gene family. Its importance in development and in DiGeorge syndrome (DGS) was revealed through a search for DGS candidate genes using engineered segmental deletions in the mouse (Lindsay et al., 1999; Lindsay et al., 2001; Merscher et al., 2001) and single gene knockouts (Jerome and Papaioannou, 2001; Lindsay et al., 2001; Merscher et al., 2001). Mutational analyses in individuals have demonstrated that *TBX1* mutations can indeed cause the DGS phenotype (Yagi et al., 2003). In mice, *Tbx1* is expressed in pharyngeal endoderm, mesodermal core of pharyngeal arches, head mesenchyme, the secondary heart field, the otocyst and sclerotome (Chapman et al., 1996; Hu et al., 2004; Vitelli et al., 2002; Xu et al., 2004). *Tbx1* is haploinsufficient in the development of the aortic arch, thymus and parathyroids (Jerome and Papaioannou, 2001; Lindsay et al., 2001; Merscher et al., 2001; Taddei et al., 2001), and homozygous mutation causes cardiovascular abnormalities, craniofacial defects, thymic and parathyroid aplasia as well as severe ear developmental defects (Jerome and Papaioannou, 2001; Kelly et al., 2004; Moraes et al., 2005; Raft et al., 2004; Vitelli et al., 2002; Vitelli et al., 2003). Most birth defects associated with DGS and with *Tbx1* mutations in mice are thought to derive from developmental abnormalities of the embryonic pharyngeal system, which is a transient, vertebrate-specific structure. The system is composed of 'modules' (pharyngeal arches, pouches and clefts) that are added during embryogenesis in a cranial-to-caudal order. The process of 'addition' of pharyngeal arches and pouches is usually referred to as pharyngeal segmentation. Loss of *Tbx1* causes severe hypoplasia or aplasia of most pharyngeal arches (2nd-4th and 6th) and pouches (2nd-4th), and severe hypoplasia of the pharynx (Jerome and Papaioannou, 2001; Vitelli et al., 2002). The genes involved in segmentation are unknown, and whether or not *Tbx1* is a direct player in this process is unclear. The severity of the early pharyngeal phenotype of $Tbx1^{-/-}$ embryos makes it difficult, if not impossible, to establish the role of *Tbx1* in development and organogenesis of pharyngeal derivatives, and to understand whether the cardiovascular phenotype is related to the pharyngeal phenotype or due to a direct role of *Tbx1* in cardiovascular development. Tissue-specific deletion (Xu et al., 2004) and hypomorphic mutations (Hu et al., 2004; Xu et al., 2004) have partially addressed this issue. However, owing to early embryonic defects, the requirement of *Tbx1* during the development of organs affected in DGS remains mostly unclear. Here, we have used a time-course deletion of *Tbx1* during embryogenesis to map over time the role of the gene in the development of pharyngeal derivatives and cardiovascular system. We have associated this

analysis with a timed map of the fate of *Tbx1*-expressing cells to correlate phenotypic findings with gene expression. Results show distinct time windows in which *Tbx1* is required for different organs and structures, and that it has a direct role during pharyngeal segmentation. In addition, our data show that *Tbx1* is required at multiple stages during the development of the same organ or system. We propose a unifying model for the mechanism of action of *Tbx1* in various organs and systems based on regulation of cell proliferation.

Materials and methods

Mouse mutants and tamoxifen-induced Cre recombination

All the experiments involving mice were carried out according to a protocol reviewed and approved by the Institutional Animal Care and Use Committee of Baylor College of Medicine, in compliance with the USA Public Health Service Policy on Humane Care and Use of Laboratory Animals.

The following mouse mutant lines have been described previously: TgCAGG-CreER^{TM} (Hayashi and McMahon, 2002), *Tbx1*$^{flox/flox}$ and *Tbx1*$^{mcm/+}$ (Xu et al., 2004), *Tbx1*$^{+/-}$ (Lindsay et al., 2001), and R26R (Soriano, 1999). All lines were backcrossed into the C57Bl6 genetic background for at least two generations. Mice were genotyped using PCR as described in the original reports. To induce nuclear translocation of the inducible Cre, including Cre^{ERTM} and MerCreMer encoded by the CAGG-CreER^{TM} transgene and the *Tbx1*^{mcm} allele, respectively, pregnant mice were treated with single intraperitoneal injection of tamoxifen (Sigma) with a dose of 75 mg/kg body weight at the desired time points. Tamoxifen was dissolved in absolute ethanol at the concentration of 100 mg/ml and then diluted 1:10 in autoclaved sesame oil (Sigma) for injection. The excision of the loxP-flanked exon 5 of the *Tbx1* allele *Tbx1*^{flox} was evaluated as follows. Genomic DNA was extracted from whole E9.5 embryos exposed to TM for 3, 6, 12 or 24 hours and it was used as template in PCR. The PCR primers used to detect *Tbx1*^{flox} allele (Fig. 1A) are Tbx1loxP2-F (5′-cgacccttctctggcttatg-3′) and Tbx1loxP2-R (5′-aaagactcctgccc-ttttcc-3′). PCR products were separated in 1.5% agarose gel by electrophoresis and the intensity of the bands was measured using NIH image 1.63 software on digital images of the gel. The percentages of remaining *Tbx1*^{flox} allele in TgCAGGCre^{ERTM}; *Tbx1*$^{flox/+}$ mutants were calculated as the ratio of the intensity of *Tbx1*^{flox} band to that of *Tbx1*$^{+}$ band, and the values were normalized with those of *Tbx1*$^{flox/+}$ embryos. A second PCR strategy was used to evaluate the disappearance of the *Tbx1*^{flox} allele and the appearance of the *Tbx1*$^{\Delta E5}$ allele (see scheme in Fig. S1A in the supplementary material). To do this, we used a primer pair amplifying exon 5 and the flanking loxP sites, Tbx1E5-F (5′-ggccctgcctaactcagatt-3′) and Tbx1E5-R (5′-aaagactcctgccctttcc-3′).

Reverse-transcription polymerase chain reaction (RT-PCR)

We have used RT-PCR to detect residual *Tbx1* transcripts in TgCAGG-CreER^{TM}; *Tbx1*$^{flox/-}$ and control (TgCAGG-CreER^{TM}; *Tbx1*$^{flox/+}$ or *Tbx1*$^{flox/+}$) embryos after exposure to TM for 24 hours (see scheme in Fig. S1B in the supplementary material). Embryos at different stages (E9.5-E12.5) were harvested 24 hours after TM injection and total RNA was extracted from whole embryos using the Trizol reagent (Invitrogen). The concentration of RNA samples was measured using a spectrophotometer and adjusted to 100 ng/μl. cDNA was synthesized from mRNA using Superscript first-strand synthesis system (Invitrogen) with random hexamers as the primers, and then subjected to PCR amplification (30 cycles) using *Tbx1* and β-actin-specific primer pairs. The PCR primers used to examine *Tbx1* mRNA level were Tbx1mRNA_F (5′-TTTGTGCCCGTAGATGACAA-3′) and Tbx1mRNA_R (5′-AATCGGGGCTGATATCTGTG-3′).

Phenotypic analysis

E18.5 embryos were examined and photographed after manual dissection under a stereomicroscope. After formalin fixation, the great arteries were visualized by India ink injected into the left ventricle. Earlier embryos were examined under the stereomicroscope, fixed and paraffin embedded for histological analysis. Pharyngeal arch arteries were visualized at E10.5 using intracardiac Ink injection. Embryos were then fixed and dehydrated in ethanol: water: acetic acid: chloroform (95:3:1:1) solution and cleared in methyl salicylate: benzyl benzoate (50:50) solution. β-Galactosidase activity was visualized by staining paraformaldehyde-fixed embryos with the X-gal substrate, according to standard procedures. Stained whole-mount embryos were photographed and then embedded in paraffin and cut into 10 μm histological sections. Sections were counterstained with Nuclear Fast Red. Cell proliferation was assessed by immunohistochemistry using an anti phosphorylated histone H3 antibody (Upstate Biotechnology) on sections of ethanol-fixed, paraffin-embedded E10.0 embryos. Whole-mount RNA in situ hybridization was performed as previously described (Albrecht et al., 1997) using a *Pax1* probe kindly provided by Dr R. Balling.

Results

Time-controlled Cre-mediated deletion of the *Tbx1* gene

We have used drug-induced Cre-mediated recombination to resolve the roles(s) of *Tbx1* during embryogenesis. We have previously described a *Tbx1* conditional allele (*Tbx1*^{flox}) in which exon 5, encoding part of the T-box domain, is flanked by *loxP* sites (Xu et al., 2004). Cre-induced recombination of this allele generates the allele *Tbx1*$^{\Delta E5}$, which is functionally null. To drive Cre recombinase expression, we used a transgenic mouse line expressing ubiquitously a tamoxifen-inducible Cre^{ERTM} protein (Hayashi and McMahon, 2002). This line is hereafter referred to as TgCAGG-CreER^{TM}. We tested TgCAGG-CreER^{TM}-induced recombination of the *Tbx1*^{flox} allele by crossing TgCAGG-CreER^{TM} mice with *Tbx1*$^{flox/flox}$ mice. We treated pregnant females with a single intraperitoneal injection of tamoxifen (TM) at 75 mg/kg body weight. We harvested embryos 3, 6, 12 and 24 hours after injection. Injections were timed so that all embryos were harvested at embryonic (E) day 9.5. We used a PCR strategy on whole embryo genomic DNA to evaluate the residual (undeleted) *Tbx1*^{flox} allele after TM injection, as illustrated in Fig. 1A,B. Results showed that after 3 hours, ~28% of the floxed allele has been excised, and at 24 hours no floxed allele was detected in most embryos (Fig. 1B,C). We have also used an alternative PCR strategy to evaluate recombination, results were similar (see Fig. S1A in the supplementary material). To establish whether *Tbx1* transcripts were also depleted after 24 hours of TM exposure in TgCAGG-CreER^{TM};*Tbx1*$^{flox/-}$ embryos, we have performed RT-PCR on whole embryo RNA at different stages (E9.5, E10.5, E11.5 and E12.5). Results showed undetectable or very low level of *Tbx1* transcript at all stages tested (see Fig. S1B in the supplementary material). To establish whether the TgCAGG-CreER^{TM}-induced recombination is homogeneously distributed in the tissues of the pharyngeal apparatus, we examined TgCAGG-CreER^{TM};R26R E9.5 and E10.5 embryos after 24 hours exposure to TM. Results showed homogeneous recombination (as detected by X-gal staining) in the

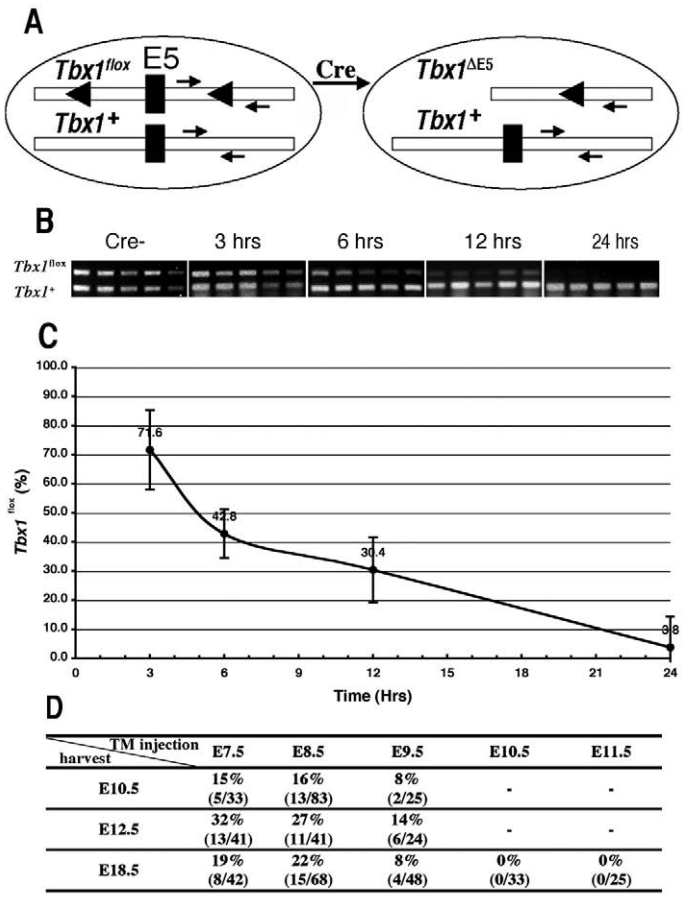

TM injection / harvest	E7.5	E8.5	E9.5	E10.5	E11.5
E10.5	15% (5/33)	16% (13/83)	8% (2/25)	-	-
E12.5	32% (13/41)	27% (11/41)	14% (6/24)	-	-
E18.5	19% (8/42)	22% (15/68)	8% (4/48)	0% (0/33)	0% (0/25)

Fig. 1. Cre-mediated recombination of the Tbx1^{flox} allele and effects of TM on embryonic viability. (A) Schematic of the polymerase chain reaction (PCR) strategy used to evaluate *Tbx1^{flox}* recombination. The primer pair (arrows) amplifies fragments of different lengths from the *Tbx1^{flox}* and wild-type alleles of *Tbx1$^{flox/+}$* cells but not from the *Tbx1$^{\Delta E5}$* allele (which results from Cre-mediated recombination of *Tbx1^{flox}*). (B) Representative PCR results from genomic DNA extracted from individual *Tbx1$^{flox/+}$* embryos (controls, Cre-) and TgCAGG-CreER^{TM};*Tbx1$^{flox/+}$* embryos exposed to TM in utero for the time indicated. There is progressive fading of the *Tbx1^{flox}* amplicon. (C) The plot indicates the progressive decrease in the intensity (percentage) of the *Tbx1^{flox}* amplicon compared with the *Tbx1^{+}* amplicon. Each point is the average of measurements from 12-17 embryos. Error bars indicate standard deviation. (D) Numbers of dead embryos at various harvest stages after TM injection at the time points indicated.

pharyngeal apparatus (see Fig. S1C in the supplementary material). Overall, these results indicate that the induction of *Tbx1^{flox}* deletion is fast, progressive and leads to essentially ubiquitous deletion within 24 hours. TM can cause embryonic lethality (Fig. 1D). However, all the wild-type embryos exposed to a single dose of TM and examined at E10.5, E12.5 and E18.5 (n=35, 16, and 39, respectively), were grossly normal. Hence, under the conditions used, exposure to TM did not cause abnormalities that may confound phenotypic analysis.

Time-based dissection of the *Tbx1* mutant phenotype

We crossed TgCAGG-CreER^{TM};*Tbx1$^{+/-}$* mice (Lindsay et al., 2001) with *Tbx1$^{flox/flox}$* mice in order to perform a time course inactivation of *Tbx1*. Pregnant females were injected with a single dose of TM at E7.5, E8.5, E9.5, E10.5 or E11.5, and we examined the fetuses at E18.5. Results (Fig. 2A,B) indicated that different organs and structures have distinct time requirements, but at no injection time point were the fetuses normal. Injection of TM at E7.5 recapitulated the germ line homozygous mutant phenotype, providing a functional confirmation that induced somatic recombination of the *Tbx1* gene with this system is sufficient to generate a null phenotype. The two major components of the cardiovascular abnormalities in *Tbx1* mutants (Vitelli et al., 2002), namely aortic arch patterning defects (in *Tbx1$^{+/-}$* and *Tbx1$^{-/-}$* mutants) and cardiac outflow tract (OFT) defects (mainly in *Tbx1$^{-/-}$* mutants) had distinct time-requirements (Fig. 2A, Fig. 3A-D). *Tbx1$^{+/-}$* animals exhibited aortic arch patterning abnormalities owing to defects of the 4th pharyngeal arch arteries (PAAs) (Jerome and Papaioannou, 2001; Lindsay and Baldini, 2001; Merscher et al., 2001; Vitelli et al., 2002). Injection of ink into the heart of E10.5 Tg-CAGG-CreER^{TM};*Tbx1$^{flox/+}$* embryos exposed to TM at E7.5 demonstrated that heterozygous deletion of *Tbx1* at this time point causes 4th PAA hypoplasia (Fig. 3E). Exposure to TM at E8.5 of embryos with the same genotype resulted in normal or only mildly hypoplastic 4th PAAs (Fig. 3F, compare with 3G). Thus, the 4th PAA haploinsufficiency phenotype is due to an early requirement for *Tbx1* that precedes the morphological appearance of the arteries, which occurs after E9.5.

Of the phenotypic abnormalities assessed in this study, clefting of the secondary palate is the only one that occurred after *Tbx1* ablation at E11.5 (Fig. 2A and Fig. 4F,G). Thus, clefting in these mutants is not due to early abnormalities of 1st pharyngeal arch patterning, which are present in *Tbx1$^{-/-}$* embryos (Kelly et al., 2004), but most likely to a role of *Tbx1* in secondary palatogenesis, which occurs from approximately E12.5.

Timed fate mapping of *Tbx1*-expressing cells

We used the *Tbx1^{mcm}* allele (Xu et al., 2004), which carries a cDNA encoding a tamoxifen-inducible Cre recombinase (Verrou et al., 1999) knocked into the *Tbx1* allele, to obtain a timed fate map of *Tbx1*-expressing cells. *Tbx1^{mcm}* allele is an inactivating allele for *Tbx1*. However, we have shown that *Tbx1* heterozygosity does not alter *Tbx1* expression pattern (Vitelli et al., 2002). Exposure of *Tbx1$^{mcm/+}$*;R26R (Soriano, 1999) embryos to a single dose of TM should induce recombination of the R26R allele and permanent expression of β-galactosidase in cells expressing *Tbx1* within 24-36 hours of injection [the half-life of TM is 11.9 hours (Robinson et al., 1991)] and their progeny. We thereby induced Cre recombination at different developmental stages and then harvested and stained embryos with X-gal at E10.5. Induction at E7.5 labeled, among other tissues, the endothelium of the 4th PAAs and the pharyngeal ectoderm, while induction at E8.5 or E9.5 did not (although very few, labeled ectodermal cells could be detected with induction at E8.5, Fig. 3H-J), suggesting that *Tbx1* may have a role in endothelial precursors and/or pharyngeal epithelia in the formation of the 4th PAAs.

A

TM	E7.5 (n=9*, 7)	E8.5 (n=18*, 4)	E9.5 (n=12*, 4)	E10.5 (n=5*, n=6)	E11.5 (n=7*, 11)
aortic arch* (haploinsufficiency)	abnormal (44%)	normal	normal	normal	normal
external ears	hypoplastic	normal	normal	normal	normal
OFT	PTA	PTA	normal	normal	normal
Thymus	absent	absent	small	small	normal
secondary palate	cleft	cleft	cleft	cleft	cleft (45%)

B

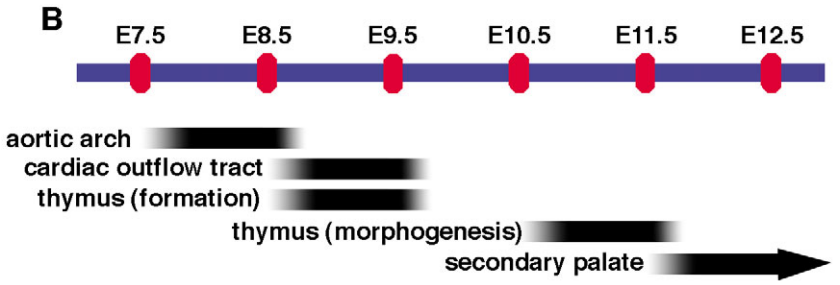

Fig. 2. Time-course deletion of *Tbx1* dissects the mutant phenotype. (A) Phenotypes scored in E18.5 TgCAGG-CreER^{TM};*Tbx1*$^{flox/-}$ or TgCAGG-CreER^{TM};*Tbx1*$^{flox/+}$ (indicated by an asterisk) embryos after in utero exposure to TM at the stages indicated. The penetrance of defects was complete, unless indicated otherwise. Aortic arch defects included interrupted aortic arch type B and aberrant origin of the right subclavian artery. OFT, cardiac outflow tract; PTA, persistent truncus arteriosus. (B) Scheme of crucial time intervals of *Tbx1* requirement for the structures or organs indicated, estimated from the results shown in A. The left extremity of each bar is set at the latest TM injection time that causes abnormalities, and the right end of the bar is set shortly after the next injection time. The gray areas in each bar indicate time required for full excision of the floxed allele (left) and possible extension of the time span (right). The arrow indicates that we do not know the end-point of the crucial time for the development of the secondary palate.

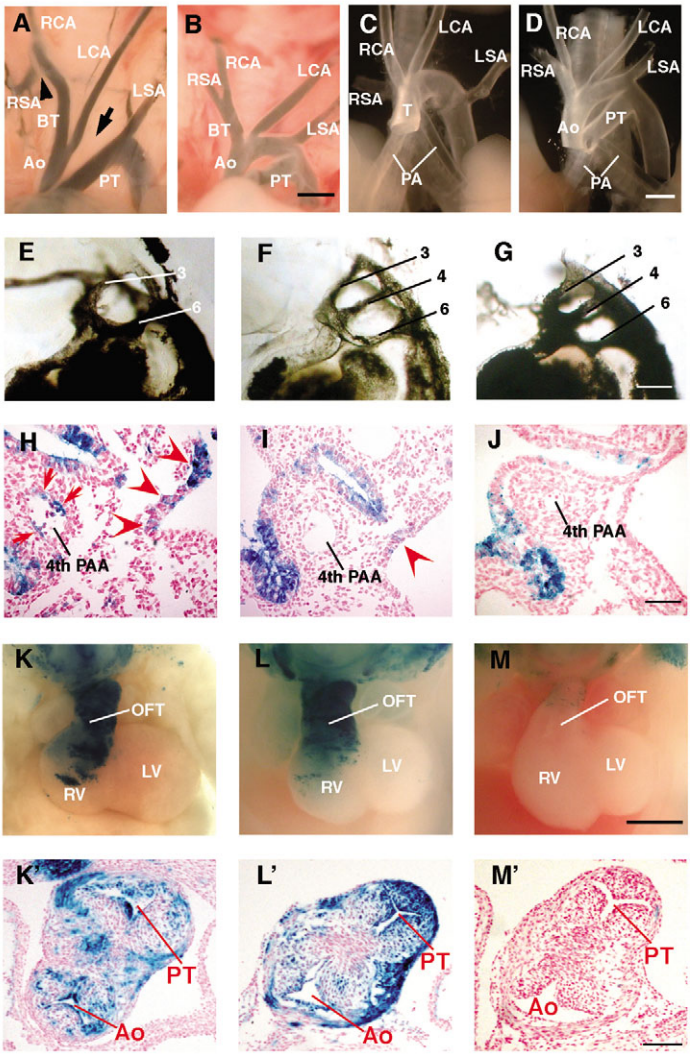

Fig. 3. Tbx1 is required early for aortic arch patterning and later for cardiac outflow tract (OFT) morphogenesis. (A) Aortic arch patterning defects in an E18.5 TgCAGG-CreER^{TM};*Tbx1*$^{flox/+}$ embryo exposed to TM at E7.5. The arrowhead indicates aberrant origin of the right subclavian artery; the arrow indicates interruption of the aortic arch, compared with normal arrangement in a *Tbx1*$^{flox/+}$ control littermate (B). (C,D) Persistent truncus arteriosus (T) in an E18.5 TgCAGG-CreER^{TM};*Tbx1*$^{flox/-}$ embryo exposed to TM at E8.5 (C), compared with normal anatomy in a TgCAGG-CreER^{TM};*Tbx1*$^{flox/+}$ littermate (D). (E-G) Intracardiac ink injection of E10.5 TgCAGG-CreER^{TM};*Tbx1*$^{flox/+}$ embryos exposed to TM at E7.5 (E), E8.5 (F) and E9.5 (G). Numbers indicate the pharyngeal arch arteries (PAAs). The 4th PAA is absent in embryos exposed to TM at E7.5 (E) and exhibits very mild hypoplasia in embryos exposed to TM at E8.5 (F); normal morphology is present in the embryo exposed at E9.5 (G). (H-J) Timed fate mapping of *Tbx1* expressing cells in E10.5 *Tbx1*$^{mcm/+}$;*R26R* embryos exposed to TM at E7.5 (H), E8.5 (I) and E9.5 (J) stained with X-gal; coronal sections, cranial is upwards. Arrowheads indicate labeling of surface ectoderm, arrows indicate labeling of endothelial cells of the 4th PAA. (K-M,K′-M′) Timed fate mapping of *Tbx1*-expressing cells in E12.5 *Tbx1*$^{mcm/+}$;R26R embryos exposed to TM at E7.5 (K,K′), E8.5 (L,L′), and E9.5 (M,M′) stained with X-gal; whole-mount preparation of the heart (K-M) and coronal section through the OFT (K′-M′) at the truncal-conal transition. RSA and LSA, right and left subclavian arteries; BT, brachiocephalic trunk; Ao, aorta; PT, pulmonary trunk; RCA and LCA, right and left common carotid arteries; PA, pulmonary arteries; RV and LV, right and left ventricles. Scale bars: 0.5 mm in B,D,M; 0.2 mm in G; 50 μm in J; 100 μm in M′.

The crucial time requirement for *Tbx1* in the development of the OFT (as determined by scoring the presence of persistent truncus arteriosus) is between E8.5 and E9.5 (Fig. 2A,B). Cell fate induction at these time points revealed that contribution of labeled cells to the OFT was very strong after induction at E8.5 (mainly myocardial and endothelial cells, as well as mesenchymal cells possibly derived from transformation of endothelial cells), but was very weak and restricted to the most distal segment of the OFT with induction at E9.5 (Fig. 3L,M). Some blue cells were also detected in the atria with induction at E8.5 (data not shown). Cell-fate mapping with induction at E7.5 produced similar results to those obtained with induction at E8.5, but we noted more labeled cells invading the right ventricle (Fig. 3K). These results are consistent with our previous data indicating a crucial role of *Tbx1* in cardiomyocyte precursors fated to the OFT (Xu et al., 2004), and they identify an OFT-specific subpopulation of cardiomyocyte precursors that migrates into the OFT between E8.5 and E9.5. The crucial time for *Tbx1* function in thymus formation also spans the E8.5-E9.5 time interval (Fig. 2A,B; Fig. 4A-C). The labeling of the OFT was more robust and extensive than previously reported with the same *Tbx1*^{mcm} line (Xu et al., 2004). We found that the induction with a single, high dose of TM (used here) produces a more robust labeling than repeated, low dose injections (Xu et al., 2004).

The thymic primordium derives from the endoderm of the 3rd pharyngeal pouch (Gordon et al., 2004) and *Tbx1* is required at this time interval for the formation of this pouch (Fig. 5K,L). In addition, timed fate mapping of *Tbx1*-expressing cells revealed a heavy contribution of labeled cells to the thymic primordia after induction at E8.5 (Fig. 4D), suggesting a cell-autonomous role for *Tbx1*. Surprisingly

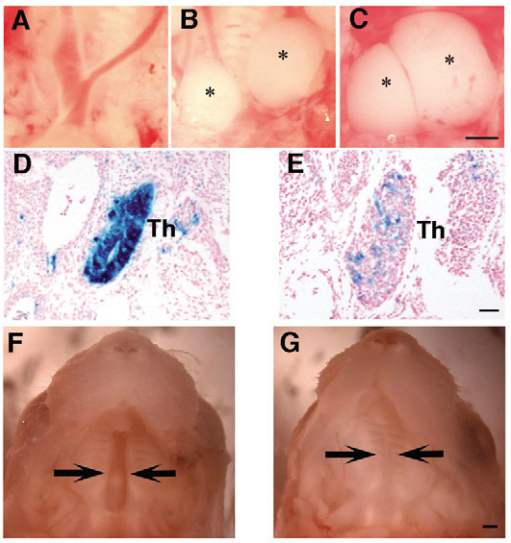

Fig. 4. Tbx1 in thymic development and palatogenesis. (A-C) Mediastinum of E18.5 TgCAGG-CreER^{TM};*Tbx1*$^{flox/-}$ embryos exposed to TM at E8.5 (A) and E9.5 (B), compared with a *Tbx1*$^{flox/-}$ control (C). Asterisks indicate thymic lobes (absent in A). Cranial is upwards. (D,E) Histological sections of X-gal stained E12.5 *Tbx1*$^{mcm/+}$;R26R embryos showing the thymic primordium (Th) after exposure to TM at E8.5 (D) and E9.5 (E). Coronal sections, cranial is up. (F,G) Secondary palate in a E18.5 TgCAGG-CreER^{TM};*Tbx1*$^{flox/-}$ embryo exposed to TM at E11.5 (F, cleft palate between the arrows), compared with that of a *Tbx1*$^{flox/-}$ control (G, normal fusion between the arrows). Cranial is upwards. Scale bars: 0.5 mm in C and G; 50 μm in E.

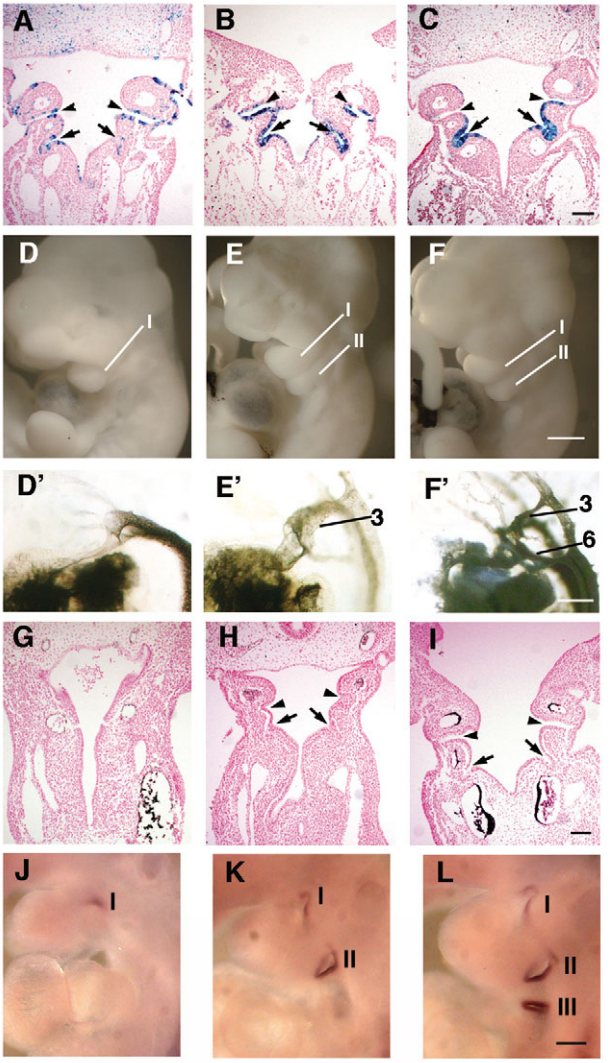

Fig. 5. Tbx1 is required during pharyngeal segmentation. (A-C) Coronal sections of X-gal stained E10.5 *Tbx1*$^{mcm/+}$;R26R embryos exposed to TM at E7.5 (A), E8.5 (B) and E9.5 (C); cranial is upwards. Arrowheads indicate the 3rd pharyngeal pouches, and arrows the 4th pharyngeal pouches. There is a progressive increase in number of labeled endodermal cells in the caudal segments. (D-F) External aspect of E10.5 TgCAGG-CreER^{TM};*Tbx1*$^{flox/-}$ embryos exposed to TM at E7.5 (D), E8.5 (E) and E9.5 (F). External abnormalities were only detected in embryos exposed to TM at E7.5 (D), which showed severe hypoplasia of the 2nd pharyngeal arch, II. (D′-F′) Intracardiac ink injection of the embryos in D-F to visualize the pharyngeal arch arteries (PAAs). Numbers indicate the PAAs. The left 6th PAA in E′ is absent, while the right one appears normal. (G-I) Coronal sections of E10.5 TgCAGG-CreER^{TM};*Tbx1*$^{flox/-}$ embryos exposed to TM at E7.5 (G), E8.5 (H) and E9.5 (I); cranial is upwards. Arrowheads, 3rd pharyngeal pouches; arrows, 4th pharyngeal pouches, black stain is residual ink injected into these embryos before paraffin embedding. (J-L) Left view of E10 TgCAGG-CreER^{TM};*Tbx1*$^{flox/-}$ embryos exposed to TM at E7.5 (J), E8.5 (K) and a *Tbx1*$^{flox/-}$ control (L) hybridized with a *Pax1* probe to identify the 1st (I), 2nd (II) and 3rd (III) pharyngeal pouches. Scale bars: 0.5 mm in F; 0.2 mm in F′ and L; 0.1 mm in C and I.

though, *Tbx1* is also required for thymic morphogenesis after E10.5, that is well after the formation of the 3rd pouch (Fig. 4B). Timed fate mapping induced at E9.5 (Fig. 4E) and E10.5 (not shown) revealed a very limited contribution of labeled cells to the thymus, suggesting different mechanisms for aplasia and morphogenesis. The thymic dysmorphism associated with *Tbx1* timed deletion at E9.5 and E10.5 is reminiscent of that associated with null mutation of *Fgf10* (Ohuchi et al., 2000; Revest et al., 2001), a target of Tbx1 (Xu et al., 2004).

Tbx1 is required during segmentation of the pharyngeal system and regulates pharyngeal endoderm expansion

Timed cell fate mapping induced at E7.5, E8.5 and E9.5 revealed a progressive 'concentration' of labeled cells in the caudal region of the pharyngeal endoderm (Fig. 5A-C). This is consistent with the described cranial-to-caudal gradient of *Tbx1* expression observed during the development of the pharyngeal system (Vitelli et al., 2002). These observations suggest a role of *Tbx1* in the process of cranial-to-caudal addition of pharyngeal arches and pouches that occurs in the E8.0-E10.5 time interval. If *Tbx1* expression is crucial for progressive addition of pharyngeal arches and pouches over time, then deletion of *Tbx1* during this process should effectively arrest it when the gene deletion occurs. To test this, we exposed TgCAGG-CreER^{TM};*Tbx1*$^{flox/-}$ embryos to TM at E7.5 or E8.5 and examined them at E10.5 when the entire complement of pharyngeal arches and pouches should have formed. Embryos exposed at E7.5 exhibited severe hypoplasia of the 2nd pharyngeal arch (Fig. 5D) and lacked the 3rd-6th arches and intervening pharyngeal pouches (Fig. 5D′,G). This phenotype is identical to that caused by germline *Tbx1*$^{-/-}$ mutation. RNA in situ hybridization showed that *Pax1,* a marker of pharyngeal pouch endoderm, is weakly expressed in the first pouch but does not identify the caudal pouches of these embryos (Fig. 5J, compare with 5L). Embryos exposed to TM at E8.5 had normally segmented 1st, 2nd, and 3rd arches and normal 1st and 2nd pouches (Fig. 5E,E′,H), but the 3rd pharyngeal pouch was not identified by *Pax1* and consisted only of a small endodermal evagination that did not approach the surface ectoderm (Fig. 5H,K). Thus, deletion of *Tbx1* at the time of 3rd pouch formation (between E9 and E9.5) resulted in developmental defects of the segments caudal to and including the 3rd pouch, but did not affect the development of segments cranial to the 3rd pouch. The addition of new arches and pouches probably requires multiple morphogenetic events, the most basic of which is the expansion of the endodermal cell population. Therefore, we tested whether loss of *Tbx1* during segmentation is associated with reduced endodermal cell proliferation in TgCAGG-CreER^{TM};*Tbx1*$^{flox/-}$ embryos exposed to TM at E8.5. We have used immunohistochemistry with an anti-phosphorylated histone H3 antibody to detect proliferating cells in E10.0 embryos. Results showed that the number of proliferating pharyngeal endodermal cells is reduced by almost 50% in TgCAGG-CreER^{TM};*Tbx1*$^{flox/-}$ embryos when compared with TgCAGG-CreER^{TM};*Tbx1*$^{flox/+}$ embryos (P=0.03) (Fig. 6A-C). By contrast, we could not detect changes in proliferation of pharyngeal mesenchyme in the same embryos (Fig. 6C). Thus, *Tbx1*, directly or indirectly, regulates the expansion by cell proliferation of the pharyngeal endoderm during segmentation (Fig. 6D).

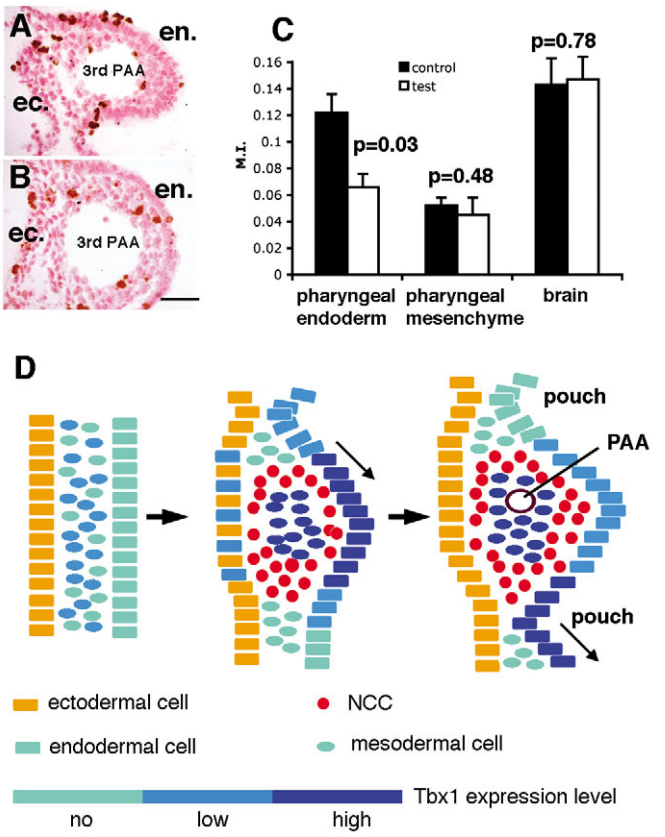

Fig. 6. Tbx1 regulates endodermal cell proliferation. (A,B) Examples of immunohistochemistry with an anti-phospho H3 antibody used to evaluate endodermal cell proliferation in E10.0 TgCAGG-CreER^{TM};*Tbx1*$^{flox/+}$ (control, A) and TgCAGG-CreER^{TM};*Tbx1*$^{flox/-}$ (test, B) embryos exposed to TM at E8.5. ec, ectoderm; en, endoderm. (C) Mitotic index (M.I.) count from at least 2000 cells per tissue per embryo; data refer to the average of three embryos per genotype; P values were calculated using the Student's t-test. Brain cells were counted as an internal control. Error bars indicate standard deviation. (D) The cartoon illustrates a model for *Tbx1* role during pharyngeal segmentation. A cranial-to-caudal 'wave' of *Tbx1* gene expression causes cranial-to-caudal expansion of the pharyngeal endoderm. This is followed by invasion of neural crest-derived cells (NCC) and formation of a new pharyngeal arch. *Tbx1* expression in pharyngeal mesoderm may also contribute to pharyngeal segmentation. PAA, pharyngeal arch artery. Scale bar: 50 μm in B.

Discussion

Induction of Cre-loxP recombination during embryogenesis

Adding a temporal dimension to the functional analysis of developmental genes can provide important information. However, this can be technically challenging, especially for mammalian embryos. We have used a Cre-*loxP* system in which the Cre recombinase is TM inducible. Our data demonstrate that the system is efficient, relatively fast responding and capable of delivering the desired deletion of the *loxP*-flanked allele in a time-controlled fashion. The

embryonic lethality caused by TM is a limitation of this approach. However, using single-injection delivery of TM, we observed a relatively low incidence of embryonic lethality associated with injections at E7.5 and E8.5, lower at E9.5 and no lethality associated with injections carried out at E10.5 and E11.5. In addition, we did not lose any pregnant female. The timing of embryo lethality-causing injection is consistent with previously reported data indicating interference of TM with placentation in rats (Sadek and Bell, 1996). With our phenotypic methods, none of the surviving embryos presented with developmental abnormalities, except for *Tbx1* mutants, and the latter only presented abnormalities previously described in these mutants. Hence, in our particular case, TM treatment did not introduce a phenotypic confounding variable.

Time-based phenotypic dissection of the DiGeorge syndrome model

The time course deletion of *Tbx1* during embryogenesis dissected most of the phenotypic abnormalities that we have tested. Data indicated that *Tbx1* is required throughout embryogenesis and that there are discrete and distinct time intervals crucial for the development of the different organs and structures affected in the model. The knowledge of these time windows provides clues as to the role of *Tbx1* in the development of different pharyngeal derivatives. For example, thymic formation required *Tbx1* at E8.5-E9.5, this did not coincide with formation of the thymic primordia (which occurs later) but with the formation of the 3rd pharyngeal pouch, from which the thymus derives (Gordon et al., 2004; Manley and Blackburn, 2003). Thus, the role of *Tbx1* in the formation of the thymus is secondary to its role in the formation of the 3rd pouch. Surprisingly, however, *Tbx1* continues to be important for thymic development also after the formation of the 3rd pouch, as demonstrated by organ dysmorphism caused by *Tbx1* deletion after E10.5. This late phenotype is more likely to be the consequence of a role of *Tbx1* in thymic organogenesis. We were also surprised by the timing of secondary palate closure requirement. It has been shown that the patterning of the first pharyngeal arch is abnormal in $Tbx1^{-/-}$ mutants (Kelly et al., 2004), therefore we speculated that cleft palate may be a consequence of these early defects. By contrast, timed-deletion data support a role of *Tbx1* in the secondary palatogenesis, which occurs between E12 and E14.5 (Kaufman and Bard, 1999).

Tbx1 is required early for aortic arch patterning, late for outflow tract septation and identifies a subset of outflow tract-specific cardiomyocyte precursors

Tbx1 loss of function affects two segments of the cardiovascular system, the aortic arch and the OFT (Vitelli et al., 2002). We have previously shown that tissue-specific deletion of *Tbx1* can separate these two groups of abnormalities (Xu et al., 2004) suggesting distinct pathogenetic mechanisms. Here, we show that *Tbx1* is required in distinct time windows for the development of the aortic arch and OFT. Counterintuitively, *Tbx1* is required early for aortic arch patterning (a relatively late process), and later for OFT growth and remodeling (a relatively early process). Our data are consistent with a role of *Tbx1* that precedes or coincides with the formation of the 4th PAAs. Our data also exclude a direct role of *Tbx1* in the remodeling or smooth muscle lining of the 4th PAAs, in contrast to hypotheses previously put forward (Kochilas et al., 2002; Lindsay and Baldini, 2001). Indeed, deletion of *Tbx1* after the 4th PAAs are formed, but before smooth muscle lining and remodeling occurs (TM injections at E8.5, E9.5 and E10.5), resulted in no phenotypic consequences for aortic arch patterning.

Timed-deletion revealed that the requirement for *Tbx1* in OFT development is restricted to a relatively late and narrow time-window (E9.0-E9.5), which is not consistent with a crucial role in the early SHF cell populations located medially to the cardiac crescent (Kelly et al., 2001; Meilhac et al., 2004; Mjaatvedt et al., 2001; Waldo et al., 2001). Rather, our findings are consistent with a crucial role of *Tbx1* in regions that provide precursors destined to the OFT at a later stage, such as the splanchnic mesoderm (Kelly et al., 2001; Mjaatvedt et al., 2001; Waldo et al., 2001). Timed cell-fate mapping showed that the crucial time window for the *Tbx1* role in OFT development coincides with expression of *Tbx1* in cells destined to populate the OFT myocardium. It is also possible that *Tbx1*-traced cells provide a cue for neural crest infiltration or outflow cushion development, once they have entered the heart tube. While several genes have been shown to mark cells of the SHF lineage [e.g. *Nkx2.5* (Stanley et al., 2002; Waldo et al., 2001; Xu et al., 2004), *Isl1* (Cai et al., 2003), and *Mef2c* (Dodou et al., 2004)], *Tbx1* is the only gene known to mark a subpopulation of cardiomyocyte precursors destined predominantly to the OFT, demonstrating the presence of regionally specified cell populations within the SHF.

Tbx1 regulates the expansion of the endoderm during pharyngeal segmentation

The embryonic pharyngeal system has a characteristic modular structure resulting from progressive addition of new segments in a cranial-to-caudal order. In $Tbx1^{-/-}$ embryos, the pharyngeal cavity is very hypoplastic, pharyngeal pouches 2-4 are not recognizable, the first is abnormal, the second pharyngeal arch is severely hypoplastic and the 3rd-6th arches are not recognizable (Jerome and Papaioannou, 2001; Kelly et al., 2004; Vitelli et al., 2002). The zebrafish *Tbx1* mutant also has similar pharyngeal defects (Piotrowski et al., 2003; Piotrowski and Nusslein-Volhard, 2000). These phenotypic observations led to hypothesize a role of *Tbx1* in pharyngeal segmentation (Baldini, 2002). The timed deletion data reported here demonstrated that *Tbx1* is required during segmentation because elimination of *Tbx1* while the segmentation is in progress effectively stops it. *Tbx1* timed deletion is followed by downregulation of the proliferative activity of endodermal cells, indicating that at least one role of *Tbx1* in segmentation concerns regulation of endodermal cell proliferation. We propose a model (Fig. 6D) in which the cranial-to-caudal wave of *Tbx1* expression would cause a wave of expansion of the pharyngeal endoderm that allows migrating neural crest-derived cells to populate (and thus shape) the pharyngeal arches. This model is also consistent with the hypothesis that the pharyngeal endoderm has a primary role in pharyngeal segmentation (Graham, 2001; Graham and Smith, 2001). However, because *Tbx1* is also expressed in pharyngeal mesoderm and, transiently, in the pharyngeal ectoderm, we cannot exclude a role for the gene in these tissue during segmentation and (or) in triggering extracellular signals required for endodermal cell proliferation.

Is downregulation of cell proliferation a general consequence of *Tbx1* loss of function?

Tbx1 mutants and individuals with DGS have complex phenotypes. One of the goals of our time-based dissection of the phenotype is to reduce complexity so that individual abnormalities can be studied more effectively. In addition, the availability of an inducible deletion system allows one to test cellular phenotypes (e.g. proliferative activity) shortly after somatic gene deletion, hence reducing the chance of possible adaptive changes that may be effected in germline mutants. We speculate that Tbx1 may have a similar role in different tissues. Our finding of reduced proliferation in the pharyngeal endoderm is consistent with the finding that tissue-specific deletion of *Tbx1* in the precursors of OFT cardiomyocytes is associated with reduced cell proliferation in the splanchnic mesoderm/secondary heart field (Xu et al., 2004). In addition, it has been shown that overexpression of *Tbx1* in the OFT causes expansion of cellularity in that organ (Hu et al., 2004). Furthermore, the inner ear of $Tbx1^{-/-}$ embryos presents a defect of otic epithelial cell expansion (Vitelli et al., 2003). Thus, expansion of specific but different cell populations may be a general mechanism of action of Tbx1. Future experiments should determine the molecular effectors that mediate the role of Tbx1 in cell proliferation.

We thank H. Sobotka, G. Ji, M. Reese and P. Terrell for valuable technical assistance; A. McMahon and P. Soriano for making available the TgCAGG-CreER^{TM} and R26R mouse lines, respectively; and R. Behringer, E. Lindsay, J. Martin, R. Schwartz and F. Vitelli for critical reading of the manuscript. This work was funded by grants HL51524, HL64832, HL67155 and DE14521 from the National Institutes of Health (to A.B.).

Supplementary material

Supplementary material for this article is available at
http://dev.biologists.org/cgi/content/full/132/19/4387/DC1

References

Albrecht, U., Eichele, G., Helms, J. A. and Lu, H. C. (1997). Visualization of gene expression patterns by in situ hybridization. In *Molecular and Cellular Methods in Developmental Toxicology* (ed. G. P. Daston), pp. 23-48. New York: CRC Press.

Baldini, A. (2002). DiGeorge syndrome: the use of model organisms to dissect complex genetics. *Hum. Mol. Genet.* **11**, 2363-2369.

Cai, C. L., Liang, X., Shi, Y., Chu, P. H., Pfaff, S. L., Chen, J. and Evans, S. (2003). Isl1 identifies a cardiac progenitor population that proliferates prior to differentiation and contributes a majority of cells to the heart. *Dev. Cell* **5**, 877-889.

Chapman, D. L., Garvey, N., Hancock, S., Alexiou, M., Agulnik, S. I., Gibson-Brown, J. J., Cebra-Thomas, J., Bollag, R. J., Silver, L. M. and Papaioannou, V. E. (1996). Expression of the T-box family genes, Tbx1-Tbx5, during early mouse development. *Dev. Dyn.* **206**, 379-390.

Dodou, E., Verzi, M. P., Anderson, J. P., Xu, S. M. and Black, B. L. (2004). Mef2c is a direct transcriptional target of ISL1 and GATA factors in the anterior heart field during mouse embryonic development. *Development* **131**, 3931-3942.

Gordon, J., Wilson, V. A., Blair, N. F., Sheridan, J., Farley, A., Wilson, L., Manley, N. R. and Blackburn, C. C. (2004). Functional evidence for a single endodermal origin for the thymic epithelium. *Nat. Immunol.* **5**, 546-553.

Graham, A. (2001). The development and evolution of the pharyngeal arches. *J. Anat.* **199**, 133-141.

Graham, A. and Smith, A. (2001). Patterning the pharyngeal arches. *BioEssays* **23**, 54-61.

Hayashi, S. and McMahon, A. P. (2002). Efficient recombination in diverse tissues by a tamoxifen-inducible form of Cre: a tool for temporally regulated gene activation/inactivation in the mouse. *Dev. Biol.* **244**, 305-318.

Hu, T., Yamagishi, H., Maeda, J., McAnally, J., Yamagishi, C. and Srivastava, D. (2004). Tbx1 regulates fibroblast growth factors in the anterior heart field through a reinforcing autoregulatory loop involving forkhead transcription factors. *Development* **131**, 5491-5502.

Jerome, L. A. and Papaioannou, V. E. (2001). DiGeorge syndrome phenotype in mice mutant for the T-box gene, *Tbx1*. *Nat. Genet.* **27**, 286-291.

Kaufman, M. H. and Bard, J. B. L. (1999). *The Anatomical Basis of Mouse Development*. San Diego: Academic Press.

Kelly, R. G., Brown, N. A. and Buckingham, M. E. (2001). The arterial pole of the mouse heart forms from Fgf10-expressing cells in pharyngeal mesoderm. *Dev. Cell* **1**, 435-440.

Kelly, R. G., Jerome-Majewska, L. A. and Papaioannou, V. E. (2004). The del22q11.2 candidate gene Tbx1 regulates branchiomeric myogenesis. *Hum. Mol. Genet.* **13**, 2829-2840.

Kochilas, L., Merscher-Gomez, S., Lu, M. M., Potluri, V., Liao, J., Kucherlapati, R., Morrow, B. and Epstein, J. A. (2002). The role of neural crest during cardiac development in a mouse model of DiGeorge syndrome. *Dev. Biol.* **251**, 157-166.

Lindsay, E. A. and Baldini, A. (2001). Recovery from arterial growth delay reduces penetrance of cardiovascular defects in mice deleted for the DiGeorge syndrome region. *Hum. Mol. Genet.* **10**, 997-1002.

Lindsay, E. A., Botta, A., Jurecic, V., Carattini-Rivera, S., Cheah, Y.-C., Rosenblatt, H. M., Bradley, A. and Baldini, A. (1999). Congenital heart disease in mice deficient for the digeorge syndrome region. *Nature* **401**, 379-383.

Lindsay, E. A., Vitelli, F., Su, H., Morishima, M., Huynh, T., Pramparo, T., Jurecic, V., Ogunrinu, G., Sutherland, H. F., Scambler, P. J. et al. (2001). Tbx1 haploinsufficieny in the DiGeorge syndrome region causes aortic arch defects in mice. *Nature* **410**, 97-101.

Manley, N. R. and Blackburn, C. C. (2003). A developmental look at thymus organogenesis: where do the non-hematopoietic cells in the thymus come from? *Curr. Opin. Immunol.* **15**, 225-232.

Meilhac, S. M., Esner, M., Kelly, R. G., Nicolas, J. F. and Buckingham, M. E. (2004). The clonal origin of myocardial cells in different regions of the embryonic mouse heart. *Dev. Cell* **6**, 685-698.

Merscher, S., Funke, B., Epstein, J. A., Heyer, J., Puech, A., Min Lu, M. M., Xavier, R. J., Demay, M. B., Russell, R. G., Factor, S. et al. (2001). TBX1 is responsible for cardiovascular defects in velo-cardio-facial/DiGeorge syndrome. *Cell* **104**, 619-629.

Mjaatvedt, C. H., Nakaoka, T., Moreno-Rodriguez, R., Norris, R. A., Kern, M. J., Eisenberg, C. A., Turner, D. and Markwald, R. R. (2001). The outflow tract of the heart is recruited from a novel heart-forming field. *Dev. Biol.* **238**, 97-109.

Moraes, F., Novoa, A., Jerome-Majewska, L. A., Papaioannou, V. E. and Mallo, M. (2005). Tbx1 is required for proper neural crest migration and to stabilize spatial patterns during middle and inner ear development. *Mech. Dev.* **122**, 199-212.

Ohuchi, H., Hori, Y., Yamasaki, M., Harada, H., Sekine, K., Kato, S. and Itoh, N. (2000). FGF10 acts as a major ligand for FGF receptor 2 IIIb in mouse multi-organ development. *Biochem. Biophys. Res. Commun.* **277**, 643-649.

Piotrowski, T. and Nusslein-Volhard, C. (2000). The endoderm plays an important role in patterning the segmented pharyngeal region in zebrafish (Danio rerio). *Dev. Biol.* **225**, 339-356.

Piotrowski, T., Ahn, D. G., Schilling, T. F., Nair, S., Ruvinsky, I., Geisler, R., Rauch, G. J., Haffter, P., Zon, L. I., Zhou, Y. et al. (2003). The zebrafish van gogh mutation disrupts tbx1, which is involved in the DiGeorge deletion syndrome in humans. *Development* **130**, 5043-5052.

Raft, S., Nowotschin, S., Liao, J. and Morrow, B. E. (2004). Suppression of neural fate and control of inner ear morphogenesis by Tbx1. *Development* **131**, 1801-1812.

Revest, J. M., Suniara, R. K., Kerr, K., Owen, J. J. and Dickson, C. (2001). Development of the thymus requires signaling through the fibroblast growth factor receptor R2-IIIb. *J. Immunol.* **167**, 1954-1961.

Robinson, S. P., Langan-Fahey, S. M., Johnson, D. A. and Jordan, V. C. (1991). Metabolites, pharmacodynamics, and pharmacokinetics of tamoxifen in rats and mice compared to the breast cancer patient. *Drug Metab. Dispos.* **19**, 36-43.

Sadek, S. and Bell, S. C. (1996). The effects of the antihormones RU486 and tamoxifen on fetoplacental development and placental bed vascularisation

in the rat: a model for intrauterine fetal growth retardation. *Br. J. Obstet. Gynaecol.* **103**, 630-641.

Soriano, P. (1999). Generalized lacZ expression with the ROSA26 Cre reporter strain [letter]. *Nat. Genet.* **21**, 70-71.

Stanley, E. G., Biben, C., Elefanty, A., Barnett, L., Koentgen, F., Robb, L. and Harvey, R. P. (2002). Efficient Cre-mediated deletion in cardiac progenitor cells conferred by a 3′UTR-ires-Cre allele of the homeobox gene Nkx2-5. *Int. J. Dev. Biol.* **46**, 431-439.

Taddei, I., Morishima, M., Huynh, T. and Lindsay, E. A. (2001). Genetic factors are major determinants of phenotypic variability in a mouse model of the DiGeorge/del22q11 syndromes. *Proc. Natl. Acad. Sci. USA* **98**, 11428-11431.

Verrou, C., Zhang, Y., Zurn, C., Schamel, W. W. and Reth, M. (1999). Comparison of the tamoxifen regulated chimeric Cre recombinases MerCreMer and CreMer. *Biol. Chem.* **380**, 1435-1438.

Vitelli, F., Morishima, M., Taddei, I., Lindsay, E. A. and Baldini, A. (2002). Tbx1 mutation causes multiple cardiovascular defects and disrupts neural crest and cranial nerve migratory pathways. *Hum. Mol. Genet.* **11**, 915-922.

Vitelli, F., Viola, A., Morishima, M., Pramparo, T., Baldini, A. and Lindsay, E. (2003). TBX1 is required for inner ear morphogenesis. *Hum. Mol. Genet.* **12**, 2041-2048.

Waldo, K. L., Kumiski, D. H., Wallis, K. T., Stadt, H. A., Hutson, M. R., Platt, D. H. and Kirby, M. L. (2001). Conotruncal myocardium arises from a secondary heart field. *Development* **128**, 3179-3188.

Xu, H., Morishima, M., Wylie, J. N., Schwartz, R. J., Bruneau, B. G., Lindsay, E. A. and Baldini, A. (2004). Tbx1 has a dual role in the morphogenesis of the cardiac outflow tract. *Development* **131**, 3217-3227.

Yagi, H., Furutani, Y., Hamada, H., Sasaki, T., Asakawa, S., Minoshima, S., Ichida, F., Joo, K., Kimura, M., Imamura, S.-i. et al. (2003). Role of TBX1 in human del22q11.2 syndrome. *Lancet* **362**, 1366-1373.